Polymer 50 (2009) 5308–5313

Contents lists available at ScienceDirect

Polymer

journal homepage: www.elsevier.com/locate/polymer

Effect of sorption behavior on transport properties of gases in polymeric membranes

Chien-Chieh Hu [a], Ywu-Jang Fu [b,*], Kueir-Rarn Lee [c,**], Ruoh-Chyu Ruaan [d], Juin-Yih Lai [c]

[a] Department of Chemical and Materials Engineering, Nanya Institute of Technology, Chung Li, 32034, Taiwan
[b] Department of Biotechnology, Vanung University, Chung-Li 32023, Taiwan
[c] R&D Center for Membr. Technol. and Department of Chemical Engineering, Chung Yuan University, Chung-Li 32023, Taiwan
[d] Department of Chemical and Material Engineering, National Central University, Chung-Li 320, Taiwan

ARTICLE INFO

Article history:
Received 26 May 2009
Accepted 12 September 2009
Available online 16 September 2009

Keywords:
Dual mode sorption
Carbonyl group
Fractional free volume

ABSTRACT

The purpose of this work was to study the relationships between the gas sorption and transport properties in polymeric membranes. The intrinsic gas transport properties: permeation, diffusion, and sorption in a series of dense membranes with various carbonyl group densities were investigated. The poly(methyl methacrylate) (PMMA), polycarbonate (PC), and cyclic olefin copolymer (COC) membranes have similar helium permeability, but the helium permeability of poly(2,6-dimethyl-1,4-phenylene oxide) (PPO) membrane was very high. The variation of permeability for these four membranes consists with their fraction free volume. In this study, a direct relationship was found between the carbonyl group density and Langmuir affinity constant. Furthermore, dependence of the fractional free volume on the membrane Langmuir capacity constant was observed.

1. Introduction

Membrane gas separation is becoming increasingly important in the separation of industrial streams. A better understanding of the fundamental issues affecting the diffusion of small molecules through glassy polymers is essential for the continued development of the property-structure relationships required for tailoring these materials to applications involving gas separation. Numerous studies on the relationship between the molecular structure of polymers and gas transport properties have been reported in an attempt to gain a better understanding of the transport mechanism [1–6]. Several general rules for the design of improved gas separation membrane materials have been identified. Increased polymer fractional free volume generally increases gas permeability [7–9], while the inhibition of polymer chain rotational and flexural mobility generally increases permselectivity [10–12].

Gas transport in polymeric membranes can be well described using the solution-diffusion mechanism [13], in which the gas molecules first dissolve at the membrane surface, then diffuse through the material due to the concentration gradient, and finally desorb at the other side of the membrane. Based on this mechanism, the permeability coefficient of a particular penetrant gas can be expressed as the product of the diffusion coefficient, D, and the solubility coefficient, S. Increasing the solubility will increase the permeability and get an attractive improvement in the membrane productivity. Solubility, therefore, is a useful variable for improving membrane productivity. Most previous studies indicated that increasing the free volume in the membrane and polymer–penetrant interactions is a useful strategy for designing membrane materials with improved gas solubility characteristics [14–17]. There have been active studies on the effect of basic substituents on the free volume and solubility in polymeric membranes [18–20]. Additionally, the relationships between the copolymer chemical structure and gas solubility coefficient were also reported [21]. Polymer backbones contain specific polar groups that promote polymer–penetrant interactions and have been found to increase gas solubility [22–24]. A co acetylacetonte containing polycarbonate membrane was examined in our laboratory [25]. It was evident that the addition of oxygen carrying molecules in the membrane would improve the membrane selectivity toward oxygen. While many researches have studied various polymeric structures for improving solubility coefficient of membrane, only a limited number of studies have systematically varied the functional group density of polymers to understand the effect of polymer–penetrant interaction on membrane solubility and permeability. In this work, we present the results of our studies on the gas transport properties for a series of membranes with various

* Corresponding author. Tel.: +886 3 4515811; fax: +886 3 4510156.
** Corresponding author. Tel.: +886 3 4535521; fax: +886 3 2654198.
E-mail addresses: fuj@msa.vnu.edu.tw (Y.-J. Fu), krlee@cycu.edu.tw (K.-R. Lee).

0032-3861/$ – see front matter © 2009 Elsevier Ltd. All rights reserved.
doi:10.1016/j.polymer.2009.09.034

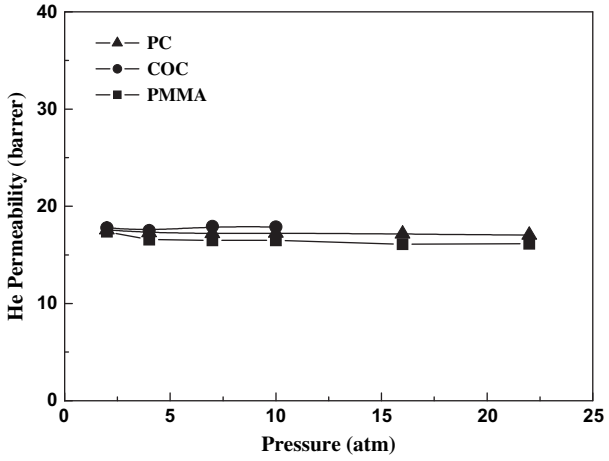

Fig. 1. The effect of upstream pressure on helium permeability for various membranes at 35 °C.

carbonyl group densities and free volume. The main goal is offering further insight into the effect of functional group density and free volume on transport and sorption behavior of polymeric membranes. We hope through such fundamental understanding will eventually lead to polymeric membranes with better gas separation performance.

2. Experimental

2.1. Materials

Polycarbonate (PC) (M_w 64000), poly(2,6-dimethyl-1,4-phenylene oxide) (PPO) (M_w 224000), and poly(methyl methacrylate) (PMMA) (M_w 996000) were purchased from the Aldrich Chemical Co. Cyclic olefin copolymer (COC) was supplied by the Ticona Co. Commercially available dichloromethane, cyclohexane, chloroform, and butylacetate were used as solvents without further purification.

2.2. Preparation of membranes

The PMMA, PC, COC, and PPO membranes were prepared using butylacetate, dichloromethane, cyclohexane and chloroform, respectively. A casting solution consisting of polymer at 15 wt% was cast onto a glass plate to a thickness of 600 μm. The solvent was then allowed to evaporate slowly under ambient conditions for 24 h. The solid PC, COC, and PPO membranes were dried in a vacuum oven at 110 °C for 24 h to remove the last traces of residual solvent. The trace PMMA membrane solvent was removed by heating the membrane at 80 °C for 24 h. The mean thickness of the membrane was measured using a micrometer and was based on an average of at least 25 points on the membrane. All membranes were between 50 and 70 μm thick.

Table 1
Physical properties and helium permeability of PMMA, PC, COC, and PPO membranes.

Membrane	T_g (°C)	Carbonyl group density (10^{-2} mol/cm^3)	Density (g/cm^3)	P_{He} (Barrer)
PMMA	105	1.21	1.209	17.4
PC	149	0.47	1.193	17.6
PPO	212	0	1.077	394.1
COC	160	0	1.045	17.8

Table 2
The long-lived components of PAL spectra of four membranes.

Membrane	τ_3 (ns)	I_3 (%)	R (Å)	FFV (%)
PMMA	2.08	21.19	2.92	3.99
PC	2.15	26.74	2.98	5.34
COC	2.23	20.62	3.05	4.41
PPO	2.69	28.45	3.41	8.5

2.3. Characterization

A Perkin-Elmer DSC7 differential scanning calorimeter was used to measure the glassy transition temperature, T_g, of the membrane at a heating rate of 10 °C min^{-1}.

The specific technique adapted to measuring the free volume of polymers is positron annihilation lifetime (PAL). For polymeric applications, ortho-positronium (o-Ps) lifetime and its probability are related to the free-volume holes size and fraction, respectively. The positron annihilation lifetimes of dense membranes were determined by detecting the prompt γ-rays (1.28 MeV) from the nuclear decay that accompanies the emission of a positron from the ^{22}Na radioisotope and the subsequent annihilation γ-rays (0.511 MeV). A fast–fast coincidence circuit of PAL spectrometer with a lifetime resolution of 260 ps as monitored by using a ^{60}Co source was used to record all PAL spectra. Each spectrum was collected to a fixed total count of 1×10^6. All of the PAL spectra were analyzed by a finite-term lifetime analysis method using the PATFIT program. The shortest lifetime ($\tau_1 \approx 0.12$ ns) is the lifetime of p-Ps, the intermediate lifetime ($\tau_2 \approx 0.4$ ns) is due to free positron annihilation, and the long lifetime ($\tau_3 \approx 1$–3 ns) is due to o-Ps annihilation. In the current PAL method, we employ the results of o-Ps lifetime to obtain the mean free-volume hole radius by the following semiempirical equation [26]:

$$\tau_3 = \frac{1}{2}\left[1 - \frac{R}{R_0} + \frac{1}{2\pi}\sin\left(\frac{2\pi R}{R_0}\right)\right]^{-1} \quad (1)$$

where τ_3 (o-Ps lifetime) and R (hole radius) are expressed in ns and Å, respectively. R_0 is equal to $R + \Delta R$, where ΔR is a fitted empirical electron layer thickness (=1.66 Å). The relative intensity of o-Ps annihilation lifetime, I_3, is related to the fractional free volume by the following empirical equation:

$$\mathrm{ffv} = CV_f I_3 \quad (2)$$

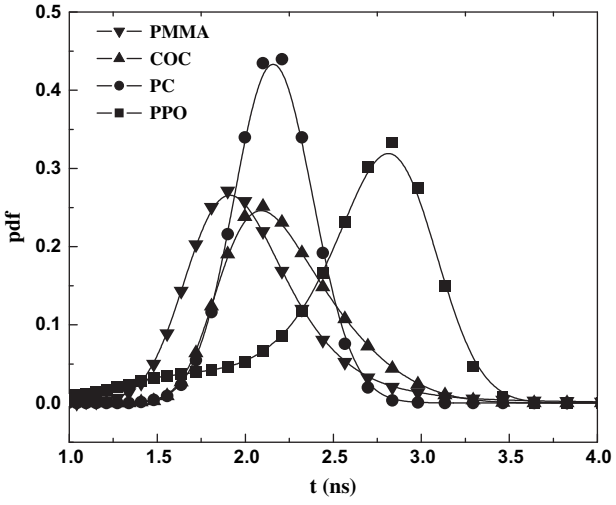

Fig. 2. The lifetime (τ_3) distributions for PMMA, COC, PC, and PPO membranes.

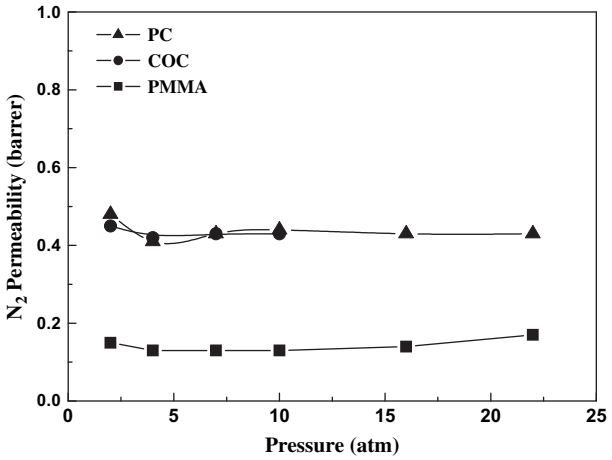

Fig. 3. The effect of upstream pressure on nitrogen permeability for PMMA, COC, PC, and PPO membranes at 35 °C.

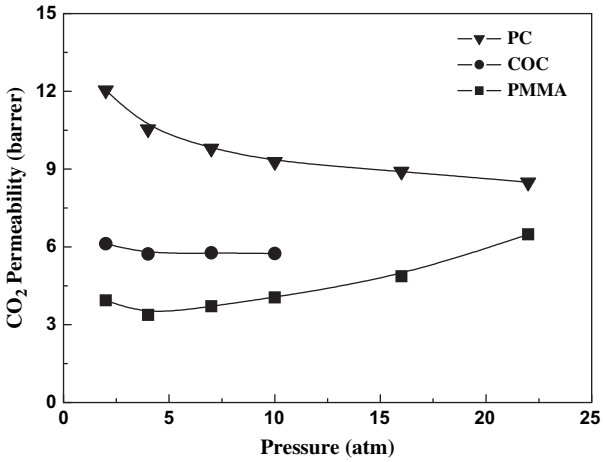

Fig. 5. The effect of upstream pressure on carbon dioxide permeability for PMMA, COC, PC, and PPO membranes at 35 °C.

where ffv is the fractional free volume and V_f is the volume (Å^3) of free-volume holes calculated from R from Eq. (1). C is an empirical constant determined from the specific volume data. Continuous lifetime distributions were obtained using the computer program MELT. This program employs a maximum entropy principle and does not need a reference spectrum to deconvolute PAL spectra as the other program, CONTIN, does.

2.4. Permeation study

A gas permeation analyzer (Yanaco GTR10) was used to measure the pure gas permeability coefficients for the polymeric membranes to He, O_2, N_2, and CO_2. The tests were carried out under isothermal conditions at 35 °C (±0.5 °C). Permeability is usually expressed as barrer (10^{-10} (cm^3(STP) cm)/(cm^2 s cmHg)). The ideal selectivity was calculated based on the ratio of the permeability coefficients:

$$\alpha_{A/B} = P_A/P_B \quad (3)$$

where P_A and P_B are the permeability coefficients of pure gases A and B. The gas sorption measurement was made using a microbalance (Cahn model D202 microbalance) to determine the amount of gas absorbed.

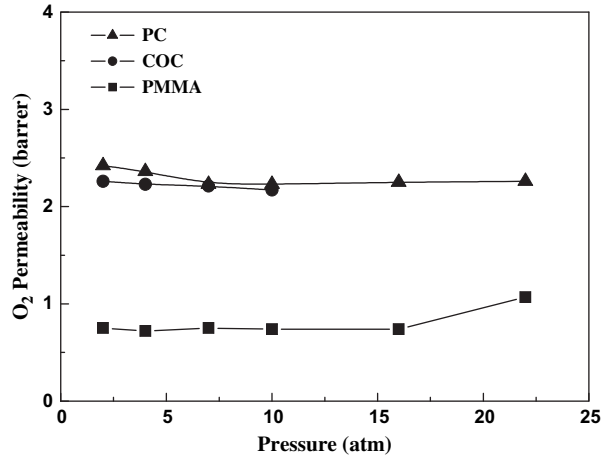

Fig. 4. The effect of upstream pressure on oxygen permeability for PMMA, COC, PC, and PPO membranes at 35 °C.

3. Results and discussion

3.1. Gas permeation behavior of dense membranes

The relationship between the chemical structure of the polymer and membrane transport properties was always the interest of study. However, the role of gas sorption on permeation has never been clearly demonstrated. To study the relations of free volume, polar group and solubility coefficient, we tried to obtained membranes with close free volume but different chemical structures. Therefore, we prepared PMMA, PC, and COC from various solvents and chose membranes with close free volumes for this study. Furthermore, the PPO membrane has very different free volume than the others and was used to survey the free volume effect on the solubility coefficient. Fig. 1 presents the He permeability of the PMMA, PC, and COC membranes at 35 °C as a function of the upstream pressure. The helium permeability coefficients in all of the membranes were independent of the pressure. This behavior is typical for gas permeation in glassy polymers over the moderate pressure ranges considered in other studies. Based on the data presented in Fig. 1, the permeabilities of the three membranes were very close. This indicated that three membranes could have similar He permeation paths. The PPO membrane permeability coefficient was very large compared with the three other membranes. Hence, we could not put the PPO membrane permeation data in Fig. 1. Nevertheless, the relationship between the permeability coefficient and pressure exhibited the same trend as the other membranes.

Table 3
Pure gas permeability, diffusivity and solubility at 10 atm and 35 °C.

Membrane	Gas	P	D	S
PMMA	O_2	0.74	4.35	0.13
	N_2	0.13	1.86	0.05
	CO_2	4.05	2.2	1.40
PC	O_2	2.22	8.54	0.20
	N_2	0.44	2.59	0.13
	CO_2	9.28	4.42	1.59
COC	O_2	2.17	12.1	0.13
	N_2	0.43	3.91	0.08
	CO_2	5.75	7.37	0.59
PPO	O_2	438.80	–	–
	N_2	483.20	–	–
	CO_2	429.20	–	–

P has units of 10^{-10} cm^3(STP) cm/cm^2 s cmHg; D has units of 10^{-8} cm^2/s; and S in cm^3(STP)/(cm^3 polymer atm).

Table 4
Ideal selectivity, diffusivity selectivity, and solubility selectivity for various membranes at 10 atm and 35 °C.

Membrane	P_{O_2}/P_{N_2}	P_{CO_2}/P_{N_2}	S_{O_2}/S_{N_2}	S_{CO_2}/S_{N_2}	D_{O_2}/D_{N_2}	D_{CO_2}/D_{N_2}
PMMA	5.7	31.2	2.4	26.3	2.3	1.2
PC	5.0	21.1	1.6	12.4	3.3	1.7
COC	5.0	13.0	1.6	7.1	3.1	1.9
PPO	0.9	0.9	–	–	–	–

P has units of 10^{-10} cm^3(STP) cm/cm^2 s cmHg; *D* has units of 10^{-8} cm^2/s; and *S* in cm^3(STP)/(cm^3 polymer atm).

By using physical characteristics we can interpret gas transport behavior in the membrane. As shown in Table 1, the density of PMMA, PC, and COC membranes was different and the magnitude of the carbonyl group density grows in the order of

$$\text{PPO} = \text{COC} < \text{PC} < \text{PMMA}.$$

It is well known that free volume and gas–polymer interaction affect the solubility coefficient of membrane. From a theoretical point of view, helium is an inert gas so we can eliminate the effect of gas–polymer interaction on solubility coefficient. Therefore, we can suppose that membranes have similar helium permeability should have similar free volume. Table 2 shows the values of the mean lifetime (τ_3), intensity (I_3), and fractional free volume (ffv) for different membranes. The results in Table 2 point out an obvious difference in free volume size and fractional free volume even if three different membranes have similar permeability. These results were not consistent with above hypothesis, so we need more information to explain the reason why membranes have similar permeability but have different free volume. The positron lifetime (τ_3) distributions of four different membranes are shown in Fig. 2. The lifetime time distribution curve of four membranes is not split into a bimodal distribution. It can be seen from Fig. 2 that the lifetime distribution curve of PC membrane has narrow and higher intensity of lifetime component, but otherwise PMMA and COC membranes reveal analogous lifetime distribution curve which have broader and lower intensity of lifetime component. If we comprehensive consider the free volume size and number, the helium permeability of PMMA, PC, and COC should be analogue. Furthermore, owing to the free volume size of PPO membrane was much big than other membranes, the helium permeability of PPO membrane was very high.

Figs. 3 and 4 present the dependence of N_2 and O_2 permeability on pressure for PMMA, PC, and COC membranes. It is evident that the PC and COC membranes have nearly the same permeability

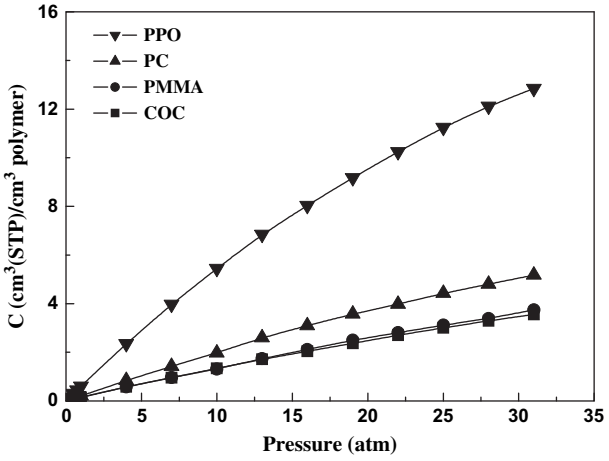

Fig. 7. Sorption isotherms of oxygen for PMMA, COC, PC, and PPO membranes at 35 °C.

coefficient. Referring to Fig. 2 and Table 2 again, PC membrane has smaller free volume size but higher fractional free volume and carbonyl group density than COC membrane. The similar N_2 and O_2 permeability observed for PC and COC membranes could be explained by the fact that the effect of fractional free volume and carbonyl group density will be offset by free volume size effect. Additionally, the permeability of the PMMA membrane was smaller than that for the PC and COC membranes. This result is consistent with the free volume and density observed from Tables 1 and 2.

Fig. 5 shows that the permeability of PC and COC membranes decrease with increased CO_2 operation pressure. Based on Figs. 3 and 4 results, we may say that the PC and COC membranes should have the same CO_2 permeability. However, the CO_2 permeability of the PC membrane was higher than COC membrane, as shown in Fig. 5. Here it should be pointed out that carbonyl group density of membrane was used to estimate the permeability value. The carbonyl group has a significant effect upon membrane permeability. There is no carbonyl group in COC membrane and so the CO_2 permeability of COC membrane was lower than PC membrane. The carbon dioxide permeability of PMMA membrane decreased with the pressure in the beginning, but continuously increased with the increase in operating pressure. The increase in gas permeability at elevated pressure was often considered a consequence of plasticization. Condensable gases plasticized the membrane and increased the polymer chain mobility at high pressure, subsequently, the permeability increased. Sanders et al. showed the plasticization

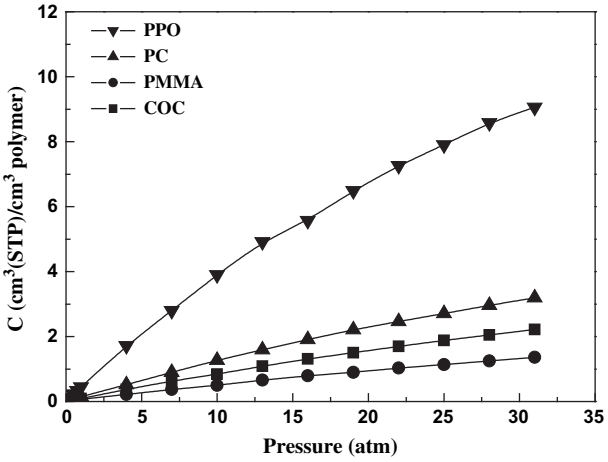

Fig. 6. Sorption isotherms of nitrogen for PMMA, COC, PC, and PPO membranes at 35 °C.

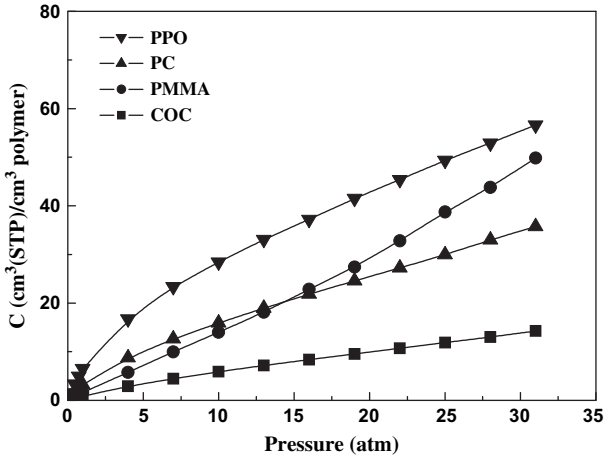

Fig. 8. Sorption isotherms of carbon dioxide for PMMA, COC, PC, and PPO membranes at 35 °C.

Table 5
Dual mode parameters for various membranes at 35 °C.

Polymer	k_D (cm^3(STP)/cm^3 atm)			C'_H (cm^3(STP)/cm^3)			b (atm^{-1})		
	O_2	N_2	CO_2	O_2	N_2	CO_2	O_2	N_2	CO_2
PMMA	0.083	0.028	1.344	2.72	1.07	0.64	0.025	0.029	0.637
PC	0.071	0.049	0.878	7.69	3.75	9.17	0.021	0.026	0.339
PPO	0.077	0.081	1.186	26.90	14.60	22.1	0.021	0.027	0.307
COC	0.062	0.036	0.359	4.15	2.56	3.64	0.021	0.024	0.165

behavior of PMMA using CO_2 at upstream pressures below 1 atm. [27]. The plasticization effect in PC and COC membranes was not obvious and it indicated that the increase in carbonyl group density is typically accompanied by a simultaneous increase in the plasticization effect.

Gas permeability, diffusivity and solubility at 10 atm are recorded in Table 3. Table 3 shows the permeability obtained in this work follow the trend.

$$P(\text{PPO}) > P(\text{PC}) > P(\text{COC}) > P(\text{PMMA}).$$

This is in the same sequence as the ffvs. It is believed that the diffusivity of a penetrant increases with the ffv of membrane. However, it is observable that the magnitude of the diffusivity of the four membranes did not follow the same trend as that for ffv. The decrease of membrane diffusivity was pronounced as the carbonyl group density in the membrane increased. This result suggested that the interaction between the carbonyl group and penetrant inhibited the penetrant diffusion in the membrane. It is believed that the membrane permeability increases with decreasing penetrant kinetic diameter. From the data in Table 3, the gas permeability changes in the following order: $P_{He} > P_{CO_2} > P_{O_2} > P_{N_2}$. This trend is consistent with the increasing kinetic diameter of the penetrants. The ideal selectivity for the four membranes is summarized in Table 4. According to Table 4 results, both O_2/N_2 and CO_2/N_2 gas pairs have higher solubility selectivity at higher carbonyl group density as a result of larger interactions between the penetrant molecules and membrane. Additionally, the ideal selectivity for a PPO membrane is under one. We can deduce that the Knudsen flow played an important role in the penetrant passing through the PPO membrane.

3.2. Sorption analysis

Pure gas sorption isotherms for N_2, O_2, and CO_2 are given in Figs. 6–8, respectively. Fig. 6 shows that with increasing pressure, the solubility decreases for all membranes tested. As reported in Fig. 6, the magnitude of the solubility grows in the order of

$$S(\text{PPO}) > S(\text{PC}) > S(\text{COC}) > S(\text{PMMA}).$$

Conversely, it was noticed that the nitrogen solubility of the membrane adopted a parallel trend with ffv. Referring to Fig. 7, the oxygen solubility of the PMMA membrane was higher and closer to that for the COC membrane. However, the ffv of COC membrane was larger than that for the PMMA membrane. From Table 1, the

Table 6
Parameters of D_D and D_H for various membranes.

Membrane	Gas	D_D (10^{-8} cm^2 s^{-1})	D_H (10^{-8} cm^2 s^{-1})
PMMA	O_2	8.6	0.5
	N_2	4.2	0.7
PC	O_2	20.8	5.7
	N_2	7.7	0.6
COC	O_2	26.5	7.4
	N_2	14.9	1.5

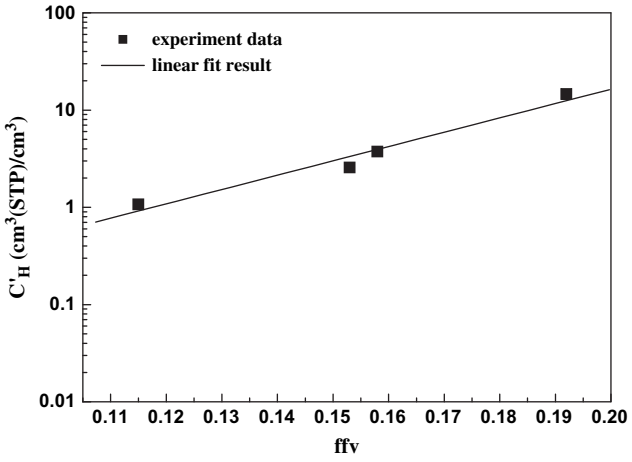

Fig. 9. Log plot of Langmuir capacity constant, C'_H vs. FFV for PMMA, COC, PC, and PPO membranes.

carbonyl group density of the PMMA membrane is markedly higher than that for the COC membrane. This indicates that the interaction between the carbonyl group and oxygen plays an important role in determining the solubility of these membranes. The solubility of CO_2 was also measured under various pressures. Fig. 8 shows that the CO_2 solubility of the PMMA membrane was still higher than that from the COC membrane. Interestingly, the CO_2 solubility in the PMMA membrane was higher than that in PC membrane at high pressure but lower at low pressure. The CO_2 solubility was favored in the presence of polar groups in the main chain. The polymer polar groups are assumed to have dipolar interactions with the polarizable carbon dioxide molecules. These interactions are stronger than the interactions between the chain segments. Thus, CO_2 breaks these interactions providing additional flexibility for the polymer chain. We attributed the plasticization behavior of PMMA to the polar and flexible pendant groups, with $-COOCH_3$, which present in the PMMA membrane. The CO_2 solubility of the PMMA membrane was higher than that in the PC membrane possibly due to the plasticization behavior of PMMA. The PPO membrane had the largest solubility on all membranes tested in this work in spite of the various gases used. This experimental finding supports the phenomenon that the higher the ffv, the more penetrant will be sorbed in the membrane and the carbonyl group effect will be ignored. Besides, it may be concluded that COC will be more

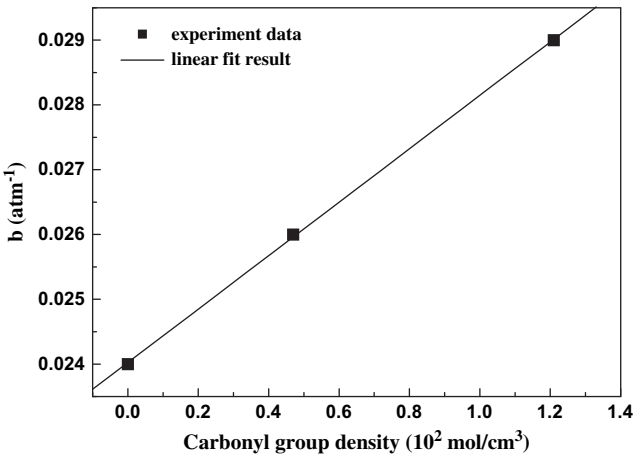

Fig. 10. Langmuir affinity constant, b, of membranes as a function of carbonyl group density.

resistant to plasticization based on its considerably lower CO_2 sorption shown in Fig. 8.

The solubility–pressure dependence for a single component is given using the dual mode model [28]

$$S = \frac{C}{p} = k_D + \frac{C'_H b}{1 + bp} \quad (4)$$

where k_D is the Henry's law constant, C'_H is the Langmuie capacity constant, and b is the Langmuir affinity constant. The C'_H term characterizes the amount of unrelaxed free volume in the glassy matrix. This allows describing the nonequilibrium nature of such materials. The b term characterizes the tendency of a given penetrant to sorb into the excess unrelaxed volume in the nonequilibrium matrix. The k_D, C'_H, and b parameters were calculated using a non-linear least squares fit of the sorption data. The results are tabulated in Table 5. The b values correlate with the carbonyl group density of the membrane. With the increase in carbonyl group density, the b values increase gradually, except for the PPO membrane. Table 5 also shows that the Langmuir capacity constant, C'_H, increases when the ffv of the membrane increases. Adopting the partial immobilization model [29], which assumes that the Langmuir's population is partially mobilized and characterized by a diffusion coefficient D_H, the permeability may be re-written as follows:

$$P = k_D D_D + D_H \frac{C'_H b}{1 + bp} \quad (5)$$

where D_D is the diffusion coefficient of Henry's population, and the D_H is the diffusion coefficient of Langmuir's population. The D_D and D_H values were obtained using a non-linear least squares fit of the permeation data after k_D, C'_H, and b are known. In agreement with the partial immobilization model concept, D_D is greater than D_H as shown in Table 6. Note that the D_D and D_H values of the COC membrane are higher than that for the PC membrane. However, the COC membrane has smaller ffv. This indicates that carbonyl group plays a more prominent role in gas diffusion inhibition through the membrane.

The dual mode model was able to describe sorption into a glassy polymer using the assumption that two regimes will enable penetrant sorption. One regime is the unrelaxed free volume of the glassy polymer. The gas absorbed into this regime can be described using the Langmuir model. C'_H represents the maximum amount of penetrant molecules sorbed into microvoids or unrelaxed free volume in the glassy polymer. Fig. 9 depicts the log of the C'_H plotted against the ffv. There is nearly a linear correlation between C'_H and the ffv of the membrane. This result suggests that gas solubility increases exponentially with ffv. Fig. 10 shows the linear correlation of the carbonyl group density with the Langmuir affinity constant, b. A high carbonyl group density does contribute to an increase in the solubility coefficient. From Figs. 9 and 10, both carbonyl group density and ffv increase the solubility of membranes. Compared the result with the data presented in Figs. 6–8. We can conclude that solubility is improved by increasing the carbonyl group density in the polymer chains of various polymers and its effect becomes more pronounced with increasing penetrant condensability.

4. Conclusion

We have studied the effect of sorption on gas separation behavior of a series of polymeric membranes that had different carbonyl group densities. The PMMA, PC, and COC membranes had the same He permeability. The PC and COC membranes had nearly the same permeability coefficients for O_2 and N_2. Membranes with similar permeability are thought to relate to ffv and free volume size distribution. The CO_2 permeability of the PC membrane was higher than that for the COC membrane. The enhanced CO_2 permeability could be associated with increased carbonyl group solubility. The solubility of the gases adopted a trend with their critical temperature. CO_2 demonstrated the highest sorption level, followed by O_2, and N_2. The Langmuir affinity constant increased with the increase in carbonyl group density, and the Langmuir capacity constant increased with the ffv. The carbonyl group plays a more prominent role in gas diffusion inhibition through the membrane.

Acknowledgement

The authors wish to sincerely thank the Ministry of Economic Affairs and the National Science Council of Taiwan, ROC, for financially supporting this project.

References

[1] Barbari TA, Koros WJ, Paul DR. J Membr Sci 1989;42:69–86.
[2] Yampolskii YP, Korikov AP, Shantarovich VP, Nagai K, Freeman BD, Masuda T, et al. Macromolecules 2001;34:1788–96.
[3] Singh A, Ghosal K, Freeman BD, Lozano AE, de la Campa JG, de Abajo J. Polymer 1999;40:5715–22.
[4] Xu ZK, Böhning M, Schultze JD, Li GT, Springer J, Glatz FP, et al. Polymer 1997;38:1573–80.
[5] Aitken CL, Paul DR, Mohanty DK. J Polym Sci B Polym Phys 1993;31:983–9.
[6] Barbari TA, Koros WJ, Paul DR. J Polym Sci B Polym Phys 1988;26:709–27.
[7] Nagelk C, Schade G, Fritsch D, Strunskus T, Faupel F. Macromolecules 2002;35:2071–7.
[8] Tanaka K, Kita H, Okano M, Okamota KI. Polymer 1992;33:585–92.
[9] Ghosal K, Freeman BD, Chern RT. Polymer 1995;36:793–800.
[10] Kim IW, Lee KJ, Jho JY, Park HC, Won J, Kang YS, et al. Macromolecules 2001;34:2908–13.
[11] Burns RL, Koros WJ. Macromolecules 2003;36:2374–81.
[12] Wang Z, Chen T, Xu J. J Appl Polym Sci 1997;64:1725–32.
[13] Paul DR, Yampol'skii YP. Polymer gas separation membranes. Boca Raton: CRC Press; 1994.
[14] Barbari TA, Koros WJ, Paul DR. J Polym Sci B Polym Phys 1988;26:729–44.
[15] Wright CT, Paul DR. Polymer 1997;38:1871–8.
[16] Zimmerman CM, Koros WJ. J Polym Sci B Polym Phys 1999;37:1235–49.
[17] Fried JR, Li W. J Appl Polym Sci 1990;41:1123–31.
[18] Mchattie JS, Koros WJ, Paul DR. J Polym Sci B Polym Phys 1991;29:731–46.
[19] Aitken CL, Koros WJ, Paul DR. Macromolecules 1992;25:3651–8.
[20] Ghosal K, Chern RT, Freeman BD, Daly WH, Negulescu II. Macromolecules 1996;29:4360–9.
[21] Nakagawa T, Nishimura T, Higuchi A. J Membr Sci 2002;206:149–63.
[22] Koros WJ. J Polym Sci B Polym Phys 1985;23:1611–28.
[23] Pixton MR, Paul DR. Polymer 1995;36:2745–51.
[24] Bos A, Pünt IGM, Wessling M, Strathmann H. J Membr Sci 1999;155:67–78.
[25] Chen SH, Lai JY, Ruaan RC, Wang AA. J Membr Sci 1997;123:197–205.
[26] Nakanishi H, Jean YC. In positron and positron chemistry. Amsterdam: Elsevier; 1998.
[27] Sander ES, Jordan SM, Subramanian R. J Membr Sci 1992;74:29.
[28] Koros WJ. J Polym Sci B Polym Phys 1980;18:981–92.
[29] Koros WJ, Paul DR. J Polym Sci B Polym Phys 1976;14:675–85.